Received: 30 August 2023 | Revised: 22 September 2023 | Accepted: 24 October 2023

DOI: 10.1002/jmr.3067

RESEARCH ARTICLE

Journal of Molecular Recognition WILEY

Identification of mitogen-activated protein kinase 7 inhibitors from natural products: Combined virtual screening and dynamic simulation studies

Bandar Alharbi[1] | Lina I. Alnajjar[2] | Hassan H. Alhassan[3] | Shama Khan[4] | Talha Jawaid[5] | Bekhzod S. Abdullaev[6,7] | Nawaf Alshammari[8] | Dharmendra Kumar Yadav[9,10] | Mohd Adnan[8] | Anas Shamsi[11]

[1]Department of Medical Laboratory Science, College of Applied Medical Sciences, University of Hail, Hail, Saudi Arabia

[2]Department of Pharmacy Practice, College of Pharmacy, Princess Nourah bint Abdulrahman University, Riyadh, Saudi Arabia

[3]Department of Clinical Laboratory Sciences, College of Applied Medical Sciences, Jouf University, Sakaka, Saudi Arabia

[4]South African Medical Research Council, Vaccines and Infectious Diseases Analytics Research Unit, Faculty of Health Science, School of Pathology, University of the Witwatersrand, Johannesburg, South Africa

[5]Department of Pharmacology, College of Medicine, Al Imam Mohammad Ibn Saud Islamic University (IMSIU), Riyadh, Saudi Arabia

[6]Department of Strategic Development, Innovation and Research, New Uzbekistan University, Tashkent, Uzbekistan

[7]Department of Oncology, School of Medicine, Central Asian University, Tashkent, Uzbekistan

[8]Department of Biology, College of Science, University of Ha'il, Ha'il, Saudi Arabia

[9]College of Pharmacy, Gachon University of Medicine and Science, Incheon, South Korea

[10]Arontier Co., Seoul, Republic of Korea

[11]Center for Medical and Bio-Allied Health Sciences Research Research, Ajman University, Ajman, United Arab Emirates

Correspondence
Anas Shamsi, Centre of Medical and Bio-Allied Health Sciences Research, Ajman University, Ajman, United Arab Emirates.
Email: anas.shamsi18@gmail.com

Funding information
Princess Nourah bint Abdulrahman University, Grant/Award Number: PNURSP2023R341

Abstract

Mitogen-activated protein kinase 7 (MAPK7) is a serine/threonine protein kinase that belongs to the MAPK family and plays a vital role in various cellular processes such as cell proliferation, differentiation, gene transcription, apoptosis, metabolism, and cell survival. The elevated expression of MAPK7 has been associated with the onset and progression of multiple aggressive tumors in humans, underscoring the potential of targeting MAPK7 pathways in therapeutic research. This pursuit holds promise for the advancement of anticancer drug development by developing potential MAPK7 inhibitors. To look for potential MAPK7 inhibitors, we exploited structure-based virtual screening of natural products from the ZINC database. First, the Lipinski rule of five criteria was used to filter a large library of ~90,000 natural compounds, followed by ADMET and pan-assay interference compounds (PAINS) filters. Then, top hits were chosen based on their strong binding affinity as determined by molecular docking. Further, interaction analysis was performed to find effective and specific compounds that can precisely bind to the binding pocket of MAPK7. Consequently, two compounds, ZINC12296700 and ZINC02123081, exhibited significant binding affinity and demonstrated excellent drug-like properties. All-atom molecular dynamics simulations for 200 ns confirmed the stability of MAPK7-ZINC12296700 and MAPK7-ZINC02123081 docked complexes. According to the molecular mechanics Poisson–Boltzmann surface area investigation, the binding affinities of both complexes were considerable. Overall, the result suggests that ZINC12296700 and ZINC02123081 might be used as promising leads to develop novel MAPK7 inhibitors. Since these compounds would interfere with the kinase activity of MAPK7, therefore, may be implemented to control cell growth and proliferation in cancer after required validations.

KEYWORDS
cancer, mitogen-activated protein kinase 7, MM-PBSA calculation, molecular dynamics simulation, natural compounds, virtual screening

1 | INTRODUCTION

Kinases are the most important component of the living system, which performs various cellular and subcellular functions like metabolism, cell signaling, protein activity regulation, and many more.[1] Kinases are essential for cellular function.[2]; a small dysfunctioning or unregulated expression of kinases may cause drastic changes inside the cell, leading to the development of multiple complex diseases, such as cancer, neurodegeneration, diabetes, and other disorders.[3] Targeted treatment focused on specific kinases can potentially restore diseases such as cancer that arise from kinase dysfunction and certain mutations. As a result, kinases have gained significant prominence as highly desirable targets for advancing anticancer medications.[4]

Mitogen-activated protein kinase 7 (MAPK7, also known as extracellular signal-regulated kinase 5 (ERK5), is a serine/threonine protein kinase mostly found in eukaryotes.[5] MAPK7 was formally known as Big MAP kinase 1 due to its large C-terminal domain, which is roughly double the C-terminal of other members of the MAPK family, imparting structurally unique character to this kinase.[6] Three spliced variants of MAPK7 have been identified, that is, ERK5a, ERK5b, and ERK5c.[7] The activation of MAPK7 involves the integration of various mechanisms, including a range of physicochemical factors such as oxidative and hyperosmolar stress, heat, and light.[8] For its activation and subsequent translocation from the cytoplasm to the nucleus, MAPK7 relies on mitogen-activated protein kinase kinase 5 (MAP2K5).[9] MAP2K5 selectively activates MAPK7 by phosphorylation event on Thr219 and Tyr221 residues in the kinase domain.[10] The kinase domain of active MAPK7 is responsible for autophosphorylation of the C-terminal tail, which amplifies MAPK7 transcription activity and ensures the retention of kinase in the nucleus.[6,11] MAPK7 is implicated in many physiological functions, including cell proliferation, differentiation, gene transcription, apoptosis, metabolism, survival, and angiogenesis.[12]

MAPK7 is ubiquitously expressed in all tissues but is notably abundant in the kidney, heart, placenta, lungs, and brain.[13] MAPK7 is a long polypeptide chain of 816 amino acids of molecular weight 102 kDa encoded by the *MAPK7* gene.[14] MAPK7 has an N-terminal region from the amino acid range 1–406, of which 55–347 belong to the protein kinase domain. The C-terminal domain contains two proline-rich regions, from 434 to 485 as PR1 and 578 to 701 as PR2, responsible for SH3 domain interaction. The region from 664 to 789 is responsible for a transcriptional activity where autophosphorylation takes place. Due to its extended C-terminal chain of around 400 amino acids, it is approximately double the size of other MAPKs.[6] The N-terminal part shows the kinase activity and the C-terminal non-kinase part shows the transcriptional activity. The N-terminal region is more than half homologous with MAPK1 and MAPK3.[13] The N-terminal region of the kinase exhibits more than 50% homology with MAPK1 and MAPK3. Specifically, the N-terminal portion of the kinase demonstrates kinase activity, while the C-terminal portion exhibits transcriptional activity.[7]

The overexpressed MAPK7 has been reported in multiple cancers such as prostate, lung, bone, colon, pancreatic, breast, and leukemia.[15] The transformation of a typically well-functioning cell into a neoplastic state is a pivotal milestone in the progression of tumor cells.[16] Consequently, MAPK7 emerges as a highly promising biological target with the potential to address malignancies by impeding the pathways implicated in tumor progression.[15] Within this framework, the inhibition of MAPK7 signifies a promising avenue for pharmacotherapy aimed at developing novel anti-proliferative therapeutics against cancer.[17]

However, a few inhibitors of MAPK7 are reported, such as BIX02188, BIX02189,[18] PD98059, and U0126.[19,20] They can inhibit MAPK7 by inhibiting its potent activator, namely, MAP2K5. The suppressing activity of these inhibitors depends upon their amount of consumption, where a higher concentration can effectively block the activation of MAPK7 via MAP2K5/ERK1/ERK2 pathways for a longer duration. XMD8-92 is another inhibitor of MAPK7 that can suppress the activity of MAPK7 via epidermal growth factor (EGF) by blocking the autophosphorylation event in the C-terminal domain.[21] Still, novel inhibitors with high specificity and efficacy are required to suppress cancer by blocking the signaling pathways associated with MAPK7's elevated expression.

With the development and advancement of modern science, structure-based virtual screening has become an efficient computational approach to drug discovery with excellent potential and specificity.[22,23] This drug discovery pipeline incorporates various bioinformatics approaches, which are very cost-effective and sustainable.[24] The complete pipeline revolves around the purely computer-based screening of a vast library of compounds to identify potent drug-like candidates with excellent binding properties.[25] In this study, the X-ray crystal structure of MAPK7 was utilized as a framework to identify its potential inhibitors. A library of ~90,000 bioactive compounds was extracted from the ZINC12 database (https://zinc12.docking.org/), and subsequently, 32,901 compounds were refined based on zero violation of Lipinski's rule of five.[26] These 32,901 compounds were docked with the Protein Data Bank (PDB) structure of MAPK7 using InstaDock, and the best 30 hits were generated based on high binding affinity. In addition, extensive screening was conducted on the characteristics of physicochemical and ADMET (absorption, distribution, metabolism, excretion, and toxicity). Consequently, the two most promising candidates, namely ZINC12296700 and ZINC02123081, were selected for further investigation. Their interaction mechanisms, encompassing hydrogen bonding, hydrophobic interactions, and other factors, were analyzed. Subsequently, a comprehensive all-atom molecular dynamics (MD) simulation lasting 200 ns was performed to gain insights into the dynamics and stability of the protein–ligand complex. To validate the findings, molecular mechanics Poisson–Boltzmann surface area (MM-PBSA) analysis was conducted.

2 | MATERIALS AND METHODS

2.1 | Computation and web resources

The virtual screening study was conducted using an HP workstation running on the Windows 10 operating system. For the all-atom MD

simulations, a Linux-based cluster was utilized. Several online resources were utilized for the analysis and data retrieval, such as UniProt,[27] RCSB PDB,[28] PubMed,[29] SwissADME,[30] PASS online server,[31] ADMETlab 2.0,[32] and ZINC database.[33] Additionally, various bioinformatics standalone software were used, like PyMOL,[34] Discovery Studio (DS) visualizer, InstaDock,[35] and XMGrace.[36]

2.2 | Receptor and ligand preparation

The X-ray crystal structure of human MAPK7 with a resolution of 1.65 Å was downloaded from RCSB PDB (PDB ID: 5BYZ). This PDB structure has the highest resolution among all available crystal structures in the PDB. The protein structure was visualized in PyMOL, and it was found that the structure contains no breaks or missing residues. Water molecules and co-crystallized molecules were removed during the preprocessing of the structure. ZINC database, a collection of naturally occurring compounds, was used to identify the potential leads against MAPK7. Lipinski's rule of five was implemented on the compounds obtained from the ZINC database. Out of ∼90,000 compounds, a set of 32,901 compounds was filtered out by qualifying Lipinski's criteria.[37]

2.3 | Molecular docking-based virtual screening

In the field of structural biology, molecular docking is a commonly employed method for predicting the potential binding conformation between a receptor and a ligand.[38] By utilizing multiple scoring functions, the docking algorithm effectively explores and identifies the optimized binding conformation, providing valuable insights into the potential docking interactions.[39] In this study, molecular docking was utilized to predict the optimal binding conformation and binding affinity of natural compounds with MAPK7. The blind docking procedure was conducted using InstaDock, an automated bioinformatics software specifically designed for high-throughput virtual screening.[35] The grid dimensions were set to blind search space where ligands were free to move and search their favorable binding sites on the protein. The search space was defined by creating a grid box with the following attribute values: $X = 81$, $Y = 59$, $Z = 77$, centered at coordinates $X = 7.704$, $Y = -33.743$, and $Z = -6.632$. The compounds were evaluated based on their binding affinity scores using the built-in scoring function of InstaDock, and hits were selected accordingly. Subsequently, interaction studies were performed with the identified hits. The resulting docked conformers were further analyzed and visualized using PyMOL and DS Visualizer. PyMOL was utilized to visualize the direct associations and polar interactions between the ligands and MAPK7, specifically focusing on those within a distance of less than 3.5 Å. The final selection of compounds was based on the interaction analysis results, which identified the residues of MAPK7 that significantly contribute to the activation loop.

2.4 | Physicochemical properties of compounds

The physicochemical properties of a chemical compound are the fundamental aspects of the pharmacological formulation.[40] A deep understanding of the physical as well as chemical nature of a compound is one of the important criteria in choosing the relevant molecule as a drug candidate. In the field of drug design and development, lead optimization is one of the crucial stages in determining a significant therapeutic for diagnosis.[41] The physicochemical attributes of a compound can be better characterized by ADMET properties. The parent library of ∼90,000 compounds was extracted from the ZINC database in PDBQT format and subjected to multiple screening steps. The very first step was filtering based on a drug-like property following Lipinski's rule of five. After the docking process, the selected compounds were further screened for PAINS filters using SwissADME (http://www.swissadme.ch/index.php). Subsequently, the compounds with PAINS patterns were deleted from the library because they have a high tendency to cause off-target side effects, making them unfavorable candidates for drug development.[42] Afterward, ADMET analysis was out to select only those hits with good ADMET profiles. The SMILES format of the obtained hits was generated using a DS Visualizer and further submitted to the ADMETlab 2.0 server to predict their pharmacokinetic properties. The compounds selected in this filter exhibited excellent ADMET properties without any toxic patterns.

2.5 | Prediction of activity spectra of substances analysis: Biological activity prediction

Prediction of activity spectra of substances (PASS) (http://www.way2drug.com/passonline/predict.php) is an online computer program that aims to predict the biochemical activity of chemical compounds.[31] It covers therapeutic properties such as mode of action, toxicity, unfavorable consequences, interaction with enzymes involved, and carriers with their impact on specific targets.[31] The PASS Online server takes only the molecular formula of the corresponding compounds as an input to predict the anticipated biological activity pattern for an endogenous drug-like substance.[43,44] We employed the PASS server to investigate the biological properties of the selected compounds. PASS analysis facilitated the identification of anti-cancer-relevant properties of the screened compounds against MAPK7. The analysis was entirely based on well-trained data sets.[43] In training datasets, "Pa" represents the compounds that belong to the category of active compounds, and "Pi" represents the compounds that belong to the category of inactive compounds. A more significant result generally has a relatively high "Pa" value.

2.6 | Molecular dynamics simulations

MD simulation is a computational technique used to simulate the behavior, dynamics, molecular geometry, and functionality of

subatomic particles within a complex system comprising proteins and ligands.[45] It plays a crucial role in drug design and discovery, providing valuable insights into the interactions and behaviors of molecules at the atomic level.[25] GROMACS simulation package was used to run MD simulations on all atoms at a controlled temperature of 300 K.[46] The entire simulation process was carried out using an HP Z840 machine. To calculate the forces between the two molecules, GROningen Molecular Simulation (GROMOS) 54A7 force field package was utilized.[47] Using the GROMOS package, we were able to model the MAPK7 system in resting as well as in bound state with the ligands, that is, ZINC12296700 and ZINC02123081.

PRODRG server was used to construct molecular topology for compounds ZINC12296700 and ZINC02123081.[48] Each system was placed 10 Å apart from each side of a cube-shaped box. The model was hydrated in the aquatic medium using the SPC216 model.[49] A required number of counterions were successfully added to maintain the electrically balanced system. Steepest descent is an iterative method employed to minimize the energy of all the systems.[50] By combining the isothermal-NVT and isobaric-NPT ensembles to positional constraints, we could attain a thermodynamically balanced state. A 200 ns simulation was conducted for each system, and time-dependent graphs were generated using GROMACS utilities.

2.7 | Principal component analysis

Principal component analysis (PCA) is a comprehensive methodology used to analyze the conformational motion of proteins and their dynamic behavior.[51] PCA is utilized to discover amino acid residues' folding dynamics and mobility. It is a statistical way of minimizing dimensionality utilizing a covariance matrix.[52] Dynamical analysis with a strong consistency of compounds binding with MAPK7 was studied using PCA on the generated simulated trajectory utilizing the integrated essential dynamic approach, which involves the computation of the covariance matrix.[53] PCA exploits explicit diagonalization of the Eigenvalues in the covariance matrix to resolve the conformational profiling of MAPK7 and its docked complexes.[54]

2.8 | MM-PBSA calculation

To further evaluate the binding analysis of ZINC02123081 and ZINC12296700 with MAPK7, the MM-PBSA method was used for the free energy calculation of all the systems.[55] The program calculates the binding energy of the protein–ligand complex based on different binding components. Various types of interactions, such as polar, non-polar, bonded, and non-bounded, were considered during the analysis. In the MM-PBSA method, the Poisson–Boltzmann concept was used to calculate the solvation energy of polar components. However, the solvation energy of non-polar components was calculated using the solvent-accessible surface area (SASA) approach. The *MMPBSA.py* Python script was used in this MM-PBSA calculation. The ensemble used to calculate binding energy was computed from the trajectory of the MD simulation.

3 | RESULTS AND DISCUSSION

3.1 | Molecular docking-based virtual screening

Virtual screening is a modern computer-assisted approach to drug discovery that entails screening a vast library of chemical compounds against a specific target protein.[25] The ZINC database, consisting of ~90,000 compounds, underwent filtration using Lipinski's rule of five. As a result, 32,901 compounds were identified and subsequently subjected to molecular docking with MAPK7 to identify potential high-affinity binding partners. The docking procedure produced log and out files containing affinity scores and docked conformers, respectively. Among the generated results, a total of 30 hits were selected based on their binding affinities and conformations, ranging from −13.4 to −11.6 kcal/mol (Table 1). The results showed that the selected compounds have a high potential to bind with MAPK7, which can be explored further to discover potential hits for drug development.

3.2 | ADMET properties of compounds

After the molecular docking analysis, the compounds underwent PAINS analysis, where no compounds exhibited PAINS patterns. Further, ADMET properties were analyzed to identify compounds that fulfill the requirements. Online web servers SwissADME and ADMETlab 2.0 were utilized to assess the ADMET properties. Among 30 compounds from the docking analysis, only two compounds showed favorable ADMET properties without any toxic patterns (Table S1). Table 2 presents the projected ADMET properties of the finally selected hits, highlighting their compliance with drug-like features and the absence of any toxic patterns. The study suggested that the selected compounds possess favorable ADMET profiles, indicating their potential utility in drug development projects.

3.3 | PASS analysis: Biological activity predictions

The PASS online server was used to investigate the biological characteristics of substances based on their molecular composition. Depending upon the projected activity range, the screening of a potential compound might be organized in the decreasing arrangement of Pa and Pi; where Pa signifies the probability of being active, and Pi signifies the probability of being inactive. The bioactivity of the compounds was predicted, keeping the cutoff value of Pa >0.7. The compounds feature antitumor properties, including antineoplastic and TP53 expression enhancers. After completing the PASS analysis, both compounds succeeded in the pharmacokinetic assessment with antineoplastic properties. The prediction was quite accurate when Pa > Pi for the two selected compounds having cancer inhibitory roles with Pa value extending from 0.675 to 0.934, as shown in Table 3. Consequently, these compounds can be considered potential leads in anticancer therapeutic development targeting MAPK7.

3.4 | Interaction analysis

Interaction analysis of MAPK7 with the selected compounds ZINC02123081 and ZINC12296700 was performed to explore their binding pattern. We have generated up to nine docked conformations for the compounds. The docked conformations showed their preferential and alternative docking positions on MAPK7 with varying affinity. For this analysis, we utilized a reference compound, 3-amino-5-[(4-chlorophenyl)amino]-N-(propan-2-yl)-1H-1,2,4-triazole-1-carboxamide, with suitable docked conformers that efficiently bind with the key residues present at the binding site of MAPK7. The binding poses of the selected compounds specifically interacting with the active site residues of MAPK7 were selected for the analysis. ZINC02123081 and ZINC12296700 were discovered to preferentially bind with MAPK7 involving several common residues such as Tyr66, Val69, Ala82, Ile61, and Asp143, where the co-crystallized inhibitor of MAPK7 interacts (PDB ID: 4QX). ZINC02123081 has strong hydrogen bonding with MAPK7 at Tyr66 and Asn187, as well as multiple additional interactions with Val69, Ala82, Lys84, Ile115, Leu137, Asp143, and Leu189. ZINC12296700 forms a hydrogen bond with MAPK7 at Tyr66, Lys84, and Ser186. In addition to hydrogen bonding, various other interactions were also formed, such as Tyr66, Val69, Ala82, Lys84, Ile115, Leu137, Asp143, and Leu189 (Figure 1). Also, this analysis strongly indicates that the compounds ZINC02123081 and ZINC12296700 have a greater affinity toward MAPK7.

The binding arrangement of ZINC02123081 and ZINC12296700 is shown in Figure 1. The binding of compounds ZINC02123081 and ZINC12296700 with the active residues present in the binding pocket of MAPK7 (Figure 1B). When the compounds come in proximity to the MAPK7 catalytic site, they overlap in a variety of ways. ZINC02123081 and ZINC12296700 bind to MAPK7 and block the cavity, exhibiting complete complementarity (Figure 1C). The study revealed that ZINC02123081 and ZINC12296700 exhibited a multitude of strong interactions with the crucial residues of MAPK7. These interactions significantly impacted the binding and stability of both

TABLE 1 Selected hits and their binding affinity toward mitogen-activated protein kinase 7.

No.	Compound ID	Affinity (kcal/mol)
1.	ZINC08789996	−13.4
2.	ZINC03845566	−13.4
3.	ZINC08876663	−13.3
4.	ZINC08791021	−12.7
5.	ZINC08789994	−12.7
6.	ZINC12902051	−12.6
7.	ZINC08790427	−12.6
8.	ZINC02159204	−12.6
9.	ZINC12882558	−12.5
10.	ZINC08876659	−12.5
11.	ZINC08790760	−12.5
12.	ZINC12878012	−12.4
13.	ZINC08790429	−12.4
14.	ZINC12902062	−12.3
15.	ZINC12885846	−12.3
16.	ZINC08877879	−12.3
17.	ZINC03843427	−12.3
18.	ZINC12866639	−12.1
19.	ZINC02096806	−12.1
20.	ZINC08918447	−12.0
21.	ZINC04044233	−12.0
22.	ZINC12296700	−11.9
23.	ZINC04222674	−11.9
24.	ZINC03846627	−11.9
25.	ZINC02137525	−11.9
26.	ZINC02120522	−11.8
27.	ZINC02113936	−11.8
28.	ZINC04235874	−11.7
29.	ZINC02123081	−11.6
30.	ZINC01123448	−11.6

TABLE 3 Selected compounds and their biological properties predicted through prediction of activity spectra of substances webserver.

Compound ID	Pa	Pi	Biological activity
ZINC12296700	0.780	0.014	Antineoplastic
	0.745	0.016	HIF1A expression inhibitor
	0.739	0.019	TP53 expression enhancer
	0.713	0.005	Antineoplastic (breast cancer)
ZINC02123081	0.934	0.004	HIF1A expression inhibitor
	0.815	0.010	TP53 expression enhancer
	0.709	0.006	MMP9 expression inhibitor
	0.675	0.017	Apoptosis agonist

TABLE 2 Absorption, distribution, metabolism, excretion, and toxicity properties of the selected compounds.

	Absorption		Distribution	Metabolism	Excretion	Toxicity
Compound ID	GI absorption (%)	Water solubility (log mol/L)	BBB permeation	CYP2D6 inhibitor	OCT2 substrate	AMES/skin sensitization
ZINC12296700	96.004	−5.431	−0.379	No	No	No
ZINC02123081	95.185	−4.693	−0.088	No	No	No

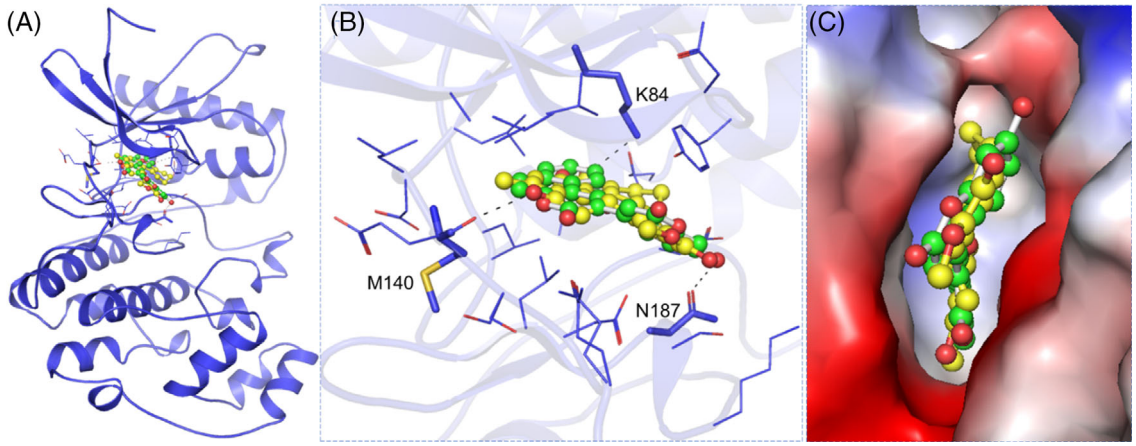

FIGURE 1 Structural representation of mitogen-activated protein kinase 7 (MAPK7) in complex with ZINC12296700 and ZINC02123081. (A) Cartoon representation of MAPK7 with the selected compounds. (B) The close interaction of MAPK7 with ZINC02123081 (green) and ZINC12296700 (yellow). (C) Surface representation of MAPK7 binding pocket occupied by the selected compounds.

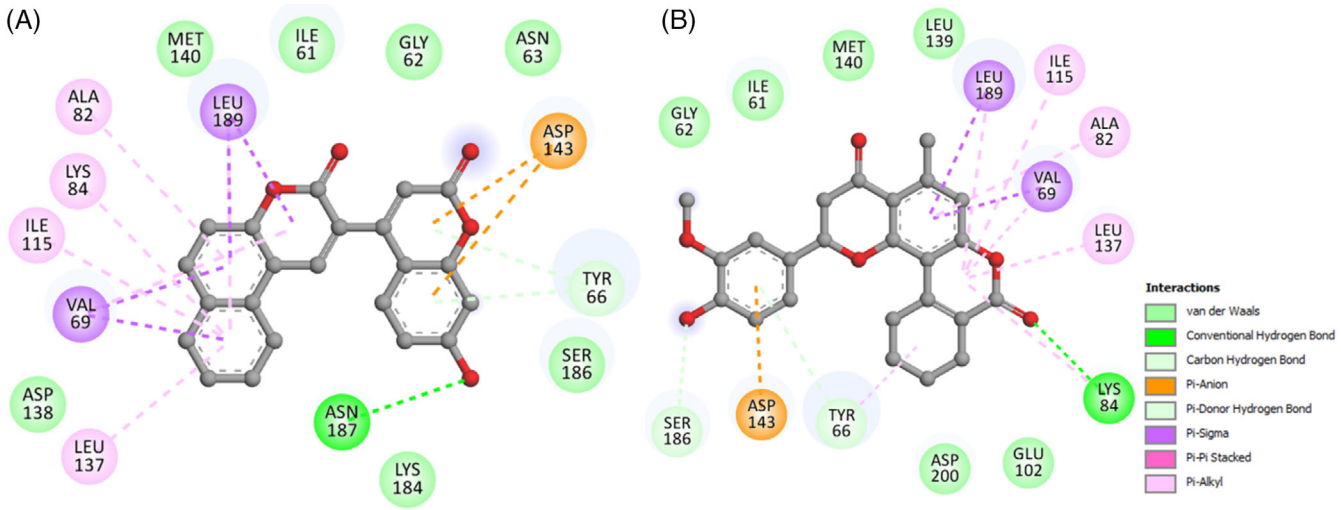

FIGURE 2 2-Dimensional plot of compounds (A) ZINC02123081 and (B) ZINC12296700 with mitogen-activated protein kinase 7.

TABLE 4 List of selected hits with IUPAC name, chemical formula, and 2-dimensional structure.

Compound ID	Compound name	Molecular formula	Structure
ZINC02123081	(2-(7-Hydroxy-2-oxochromen-4-yl)benzo[f]chromen-3-one)	$C_{22}H_{12}O_5$	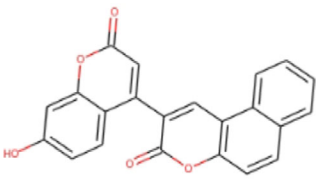
ZINC12296700	(2*S*)-2-(4-hydroxy-3-methoxyphenyl)-5-methyl-2,3,9,10,11,12-hexahydroisochromeno[3,4-h]chromene-4,8-dione	$C_{24}H_{22}O_6$	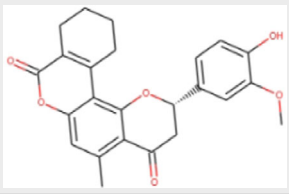

compounds with MAPK7, ultimately impeding the accessibility of ATP to MAPK7. This inhibition of ATP accessibility could lead to the suppression of MAPK7 activity.

Further, the interaction mechanism of ZINC02123081 and ZINC12296700 with MAPK7 was explored extensively. Using the DS Visualizer, the 2D models were generated, including all possible interactions of MAPK7 with ZINC02123081 and ZINC12296700 (Figure 2). The 2D plot shows how the ATP binding site of MAPK7 interacts with the compounds ZINC02123081 and ZINC12296700 (Figure 2A,B). Both compounds interact with critical residues in MAPK7's ATP binding site, that is, Lys84, and various other interactions with its kinase domain, including Tyr66, Val69, Ala82, Lys84, Ile115, Leu137, Asp143, Leu189, Asn187, and Ser186 to form a variety of interactions. According to the interaction analysis, ZINC02123081 and ZINC12296700 bind to MAPK7 at its critical sites with strong interaction. The selected hits and their 2-dimensional structure and molecular composition are shown in Table 4. Based on the interaction analysis, it is evident that ZINC02123081 and ZINC12296700 bind strongly to critical sites on MAPK7. These robust interactions influence the binding and stability of both compounds in association with MAPK7, resulting in a notable obstruction of ATP access to MAPK7. Consequently, this impediment in ATP accessibility is likely to result in the suppression of MAPK7 activity.

3.5 | MD simulations

With the rapid progress in drug development science, MD simulation has emerged as a crucial method to investigate the movement patterns of proteins over specific timeframes.[56,57] MD simulations assist in capturing the overall changes induced by conformational changes, external perturbation, complex formation, protein folding, and dynamics.[58,59] Moreover, it assists in exposing the core residues of a protein that establish some stable interactions with ligands and their mode of interaction. MD simulation of MAPK7 and the docked compounds ZINC02123081 and ZINC12296700 were conducted in an extensive aqueous environment. The simulation resulted in understanding the protein's structural dynamics and stabilization of the complex formed by MAPK7 with ZINC02123081 and ZINC12296700 in a time-dependent fashion. In a 200 ns MD simulation, MAPK7 complex with the best conformers of ZINC02123081 and ZINC12296700 in an optimum orientation were produced and exploited. The period of evaluation of numerous structural responses was tracked and assessed to better understand the behavior of MAPK7 before and after ZINC02123081 and ZINC12296700 interaction. The complete MD simulation trajectory and analysis were recorded and depicted in the form of plots and graphs generated using the XMGrace tool, as discussed in the ensuing sections.

3.5.1 | Structural deviations in MAPK7 and compactness

In the realm of MD simulations, the root mean square deviation (RMSD) serves as a useful metric for assessing the structural changes that occur in a system over time.[60] It enables the identification of specific regions within the structures that undergo evolution in comparison to their initial state.[61] By measuring RMSD, we can gain valuable insights into the extent of structural variation during a simulation.[62,63] The RMSD analysis was employed to assess the fluctuations in the backbone atoms of MAPK7. The time evolution plots of the protein were used to visually represent the changes in the backbone of the MAPK7-ZINC02123081 and MAPK7-ZINC12296700 complexes during the MD simulation. A comprehensive graph was generated to illustrate the entire simulation trajectory, allowing for an examination of the stability and consistency of the formed complexes. The binding region of the protein is highly sensitive, with even small molecules capable of inducing significant structural variations when they bind to the catalytic binding site. To evaluate the stability of MAPK7 and its complexes with ZINC02123081 and ZINC12296700, the simulation session was monitored using a time versus RMSD graph. The binding of these compounds to MAPK7 resulted in notable stability, as indicated by consistent and minor variations in the backbone atoms. In comparison to the free form of MAPK7, the ligand-bound states with ZINC02123081 and ZINC12296700 exhibited reduced variations, as depicted in the RMSD plot (Figure 3A). All three systems, namely MAPK7, MAPK7-ZINC02123081, and MAPK7-ZINC12296700, demonstrated equilibrium and stability throughout the entire 200 ns simulation trajectory (Figure 3A).

The residues' flexibility and fluctuations, measured from their mean positions, are determined by the root mean square fluctuation (RMSF) scale. During the MD simulation, RMSF calculates the local deviation of each amino acid residue. The average RMSF distribution for all three systems was approximately 10 Å. The RMSF profiles of MAPK7, MAPK7-ZINC02123081, and MAPK7-ZINC12296700 exhibit similarities, as depicted in Figure 3B. The analysis of RMSF reveals that the compounds ZINC02123081 and ZINC12296700 effectively bind to the binding pocket of MAPK7, resulting in a stable complex with minimal local variations in the amino acid residues. The overall RMSF study focuses on the significant structural changes induced in MAPK7 by the strong interaction of the compounds ZINC02123081 and ZINC12296700.

3.5.2 | Compactness of MAPK7

The radius of gyration (*Rg*) is an important characteristic used to assess the folding potential and density of a protein.[64] It measures the standard distance between the center of mass of a set of atoms and the protein's axis. The *Rg* value of a protein undergoes changes in its conformation when a ligand binds, providing insights into key features of a protein–ligand complex, including folding dynamics, conformational stability, density, and three-dimensional structure. In this study, *Rg* was employed to evaluate the compactness of MAPK7 in both its free and ligand-bound states. The presence of ligands such as ZINC02123081 and ZINC12296700 resulted in a consistently stable conformation of MAPK7 throughout the MD simulation trajectory, as evidenced by the *Rg* plot (Figure 4A). The structural dynamics and

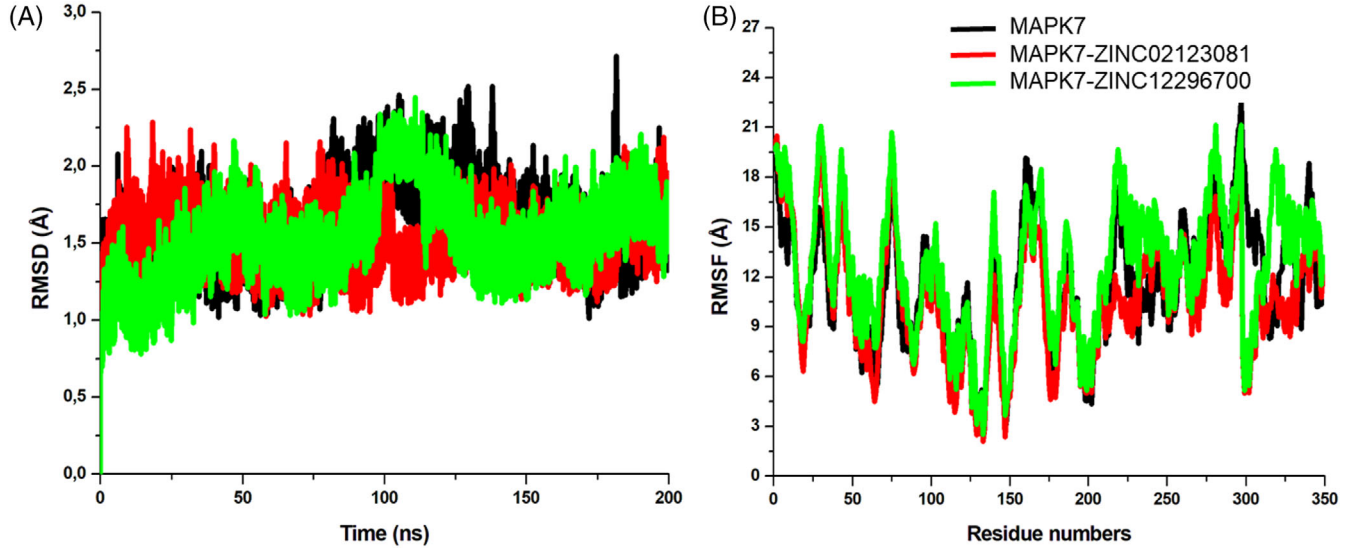

FIGURE 3 Structural dynamics of mitogen-activated protein kinase 7 (MAPK7), MAPK7-ZINC02123081, and MAPK7-ZINC12296700 complexes. (A) Root mean square deviation (RMSD) plot of MAPK7 in free and complex form over 200 ns simulation. (B) Root mean square fluctuation plot of MAPK7 in the free and bounded state obtained from 200 ns simulation trajectory. Black, red, and green represent MAPK7, MAPK7-ZINC02123081, and MAPK7-ZINC12296700, respectively.

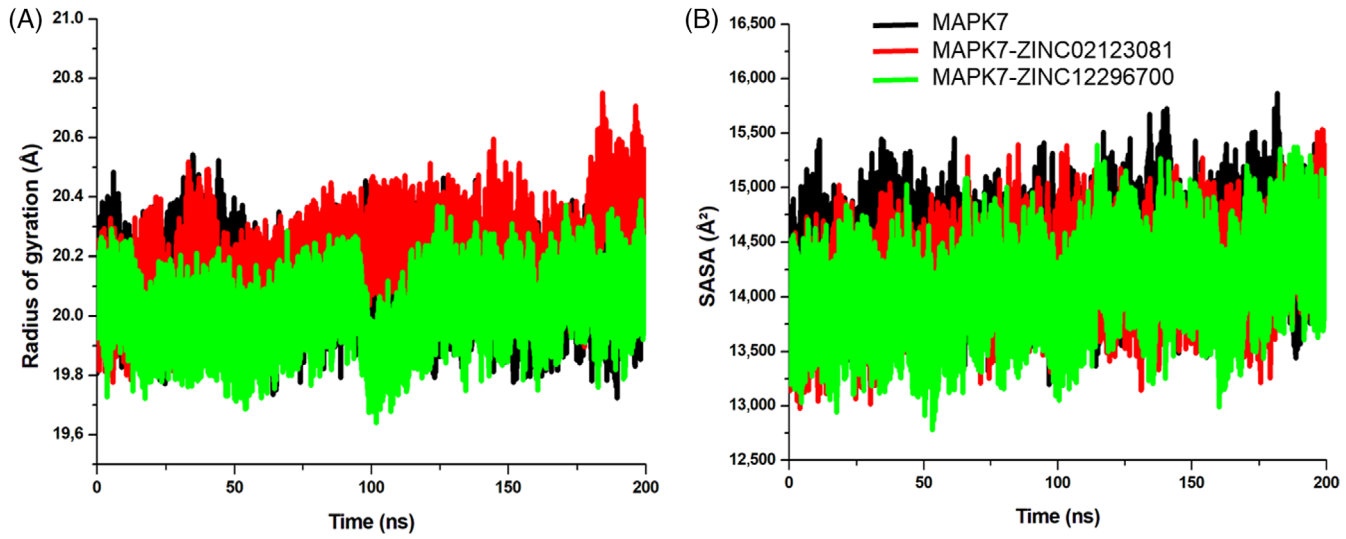

FIGURE 4 Compactness of mitogen-activated protein kinase 7 (MAPK7). (A) Rg values in Å for MAPK7 in free and ligand-bound state, calculated after a 200 ns molecular dynamics (MD) simulation trajectory. (B) Solvent-accessible surface area (SASA) value of MAPK7 with respect to time across Cα backbone in Å of all three systems across Cα backbone of all the three conditions calculated after 200 ns of MD trajectories. Black, red, and green represent MAPK7, MAPK7-ZINC02123081, and MAPK7-ZINC12296700, respectively.

folding of MAPK7 remained stable despite the binding of ZINC12296700 and ZINC02123081. The *Rg* values of MAPK7 were evenly distributed before and after the binding of ZINC12296700 and ZINC02123081, as illustrated in the plot (Figure 4A). A notably elevated *Rg* value observed in the protein–ligand complex, particularly in the case of MAPK7-ZINC02123081, suggests the occurrence of some structural adaptations throughout the simulations. However, these minor increases in *Rg* values do not significantly impact the overall protein structure.

When a solvent comes into close proximity to a protein, it engages in intimate interactions within a limited surface area defined by the protein.[65] This region of interaction is referred to as the SASA.[66] In conjunction with *Rg*, SASA is frequently employed to investigate protein structure and folding mechanisms. The analysis of SASA provides insights into the extent of protein folding and bonding. In this study, the SASA of MAPK7 was examined both before and after the binding of ZINC02123081 and ZINC12296700. Throughout the simulation, no significant changes were observed in the SASA

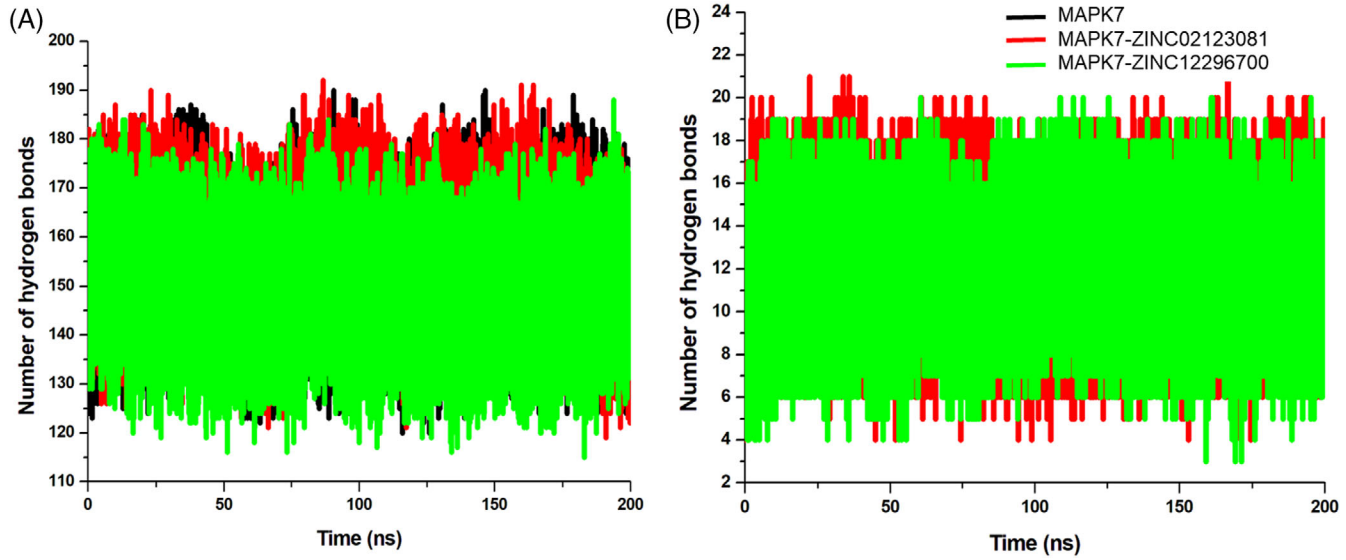

FIGURE 5 Hydrogen bond analysis. (A) Intramolecular hydrogen bonding in free mitogen-activated protein kinase 7 (MAPK7), MAPK7-ZINC02123081, and MAPK7-ZINC12296700 complexes. (B) Intermolecular bond analysis of ZINC021123081-MAPK7 and MAPK7-ZINC12296700 calculated after 200 ns molecular dynamics simulation.

values. The configuration of MAPK7 remained stable, possibly influenced by the presence of ZINC02123081 and ZINC12296700 (Figure 4B). The results obtained from the SASA analysis were consistent with the *Rg* pattern, supporting the study's overall findings.

3.6 | Dynamics of hydrogen bonds

Intramolecular hydrogen bonding plays a crucial role in maintaining proteins' three-dimensional integrity and stability.[67,68] To gain insights into the density and structural modifications of MAPK7, the intramolecular hydrogen interactions were examined before and after the binding of ZINC12296700 and ZINC02123081. Hydrogen bonding plays a crucial role in determining the packing and alignment of the protein's structure. The system's overall stability was assessed through hydrogen bond analysis of MAPK7 in both its free and bound states, with a cutoff distance of 3.5 Å. The number of hydrogen bonds formed within MAPK7 before and after the interaction with ZINC12296700 and ZINC02123081 is depicted in Figure 5. The graph illustrates that the hydrogen bonds established within MAPK7 were stable and contributed to the protein's structure and shape. As shown in Figure 5A, the intermolecular interactions formed within MAPK7 remained stable, further emphasizing the stability of the protein's internal structure.

Furthermore, a time evolution analysis of intermolecular hydrogen bonds was conducted to assess the overall stability of hydrogen bonding between MAPK7 and the compounds ZINC02123081 and ZINC12296700. This analysis provides insights into the stability of the protein–ligand complexes over time. In the complexes formed between ZINC02123081-MAPK7 and ZINC12296700-MAPK7, the average number of hydrogen bonds formed remained stable throughout the simulation (Figure 5B). This indicates that the intramolecular bonds formed within the complexes play a regulatory role in maintaining the complex's structure. Intermolecular hydrogen bonds suggest that both ZINC02123081 and ZINC12296700 have remained firmly anchored to their initial docking positions on MAPK7. These hydrogen bonds serve as a stabilizing force, effectively keeping both compounds securely within the MAPK7 binding site. Consequently, it suggests that the compounds ZINC02123081 and ZINC12296700 are unlikely to deviate from their native docking positions on MAPK7, further supporting the stability of the complex.

3.7 | Secondary structure dynamics

The structure of a protein plays a crucial role in determining its function and evolutionary relationships. The secondary structure, which includes elements such as alpha-helices and beta-sheets, influences the flexibility and folding mechanism of the polypeptide chain. These secondary structural arrangements contribute to the protein's overall three-dimensional shape. Figure 6 illustrates the variations in the secondary structural components of MAPK7 following the binding of ZINC02123081 and ZINC12296700. The graph showcases the contribution of each amino residue in generating the secondary structure throughout the experimental process. The observations indicate that the systems remained stable during the entire 200 ns simulation period. The plots demonstrate that the components of MAPK7's secondary structure were conserved in both the free state and when bound to ZINC02123081 and ZINC12296700 throughout the simulation. Table 5 provides insight into the average number of residues participating in forming the secondary structure. It was observed that the MAPK7-ZINC12296700 complex exhibited a comparatively higher value of alpha-helix and beta-sheet components when compared to the other two systems, namely

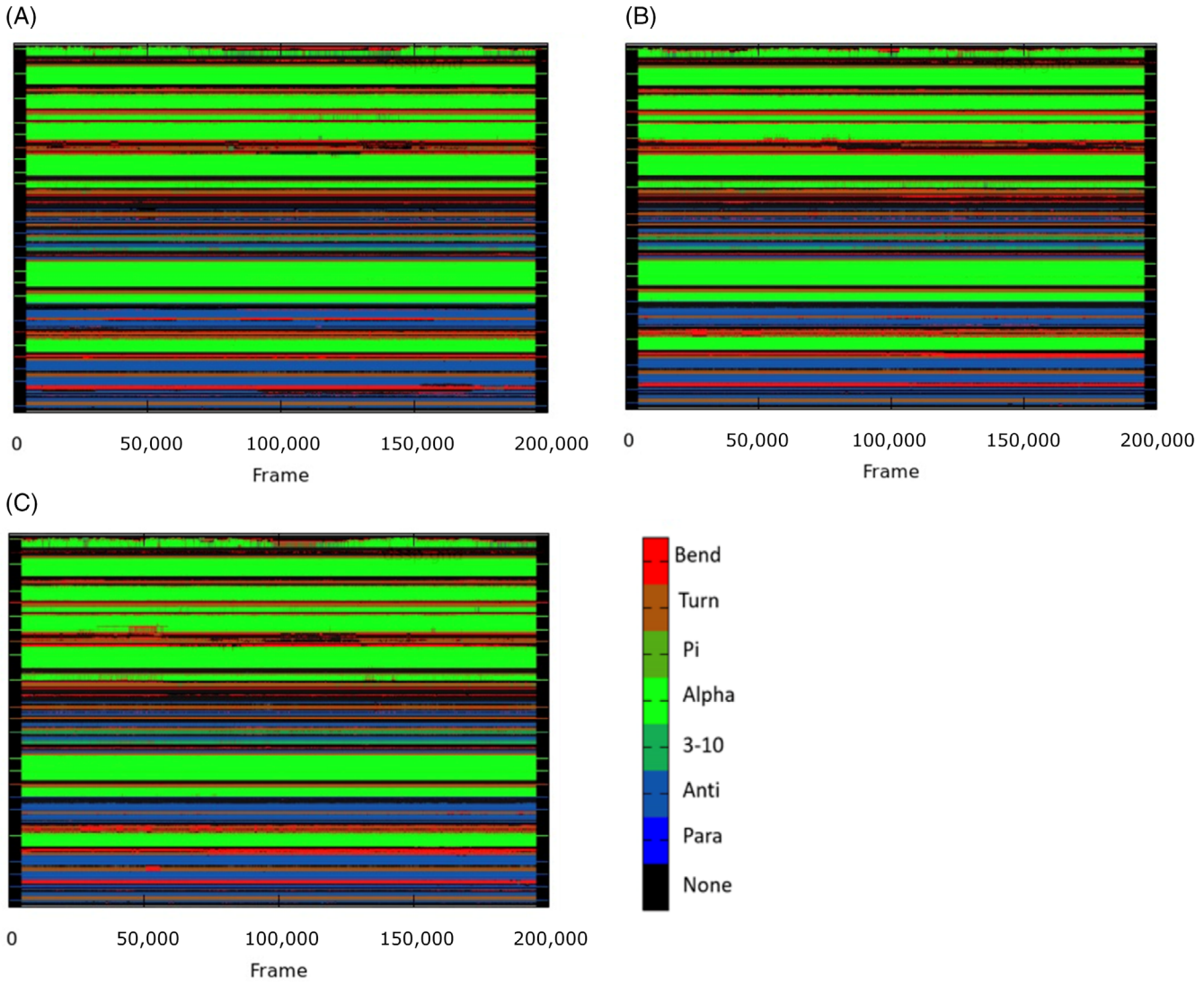

FIGURE 6 Secondary structural analysis; (A) free mitogen-activated protein kinase 7 (MAPK7) enzyme; (B) ZINC021123081-MAPK7 complex; and (C) MAPK7-ZINC12296700 complex calculated after 200 ns of molecular dynamics trajectories.

System	α	B	3_{10}-Helix	Turn	Bend	Other
MAPK7	22	27	5	11	14	25
MAPK7-ZINC021123081	24	24	6	9	8	21
MAPK7-ZINC12296700	27	26	8	13	13	27

TABLE 5 Percentage of residues contributing to the secondary structure of free mitogen-activated protein kinase 7 (MAPK7), ZINC021123081-MAPK7, and MAPK7-ZINC12296700 complexes calculated after 200 ns of molecular dynamics trajectory.

free MAPK7 and ZINC02123081-MAPK7. This suggests that the MAPK7-ZINC12296700 complex is more compact and stable than the other systems, highlighting its potential structural advantages.

3.8 | Principal component analysis

PCA is a powerful tool for simplifying and extracting meaningful information from complex protein–ligand interaction data.[69] In the study of protein–ligand interactions, it is essential to understand how protein structures change upon ligand binding. PCA can help identify and quantify these conformational changes by analyzing the principal components that capture the largest variances in protein structure.[70] The PCA in MD simulation offers a convenient method to determine the movement patterns of a protein.[51] By employing PCA, we can effectively identify the principal modes of motion exhibited by the protein during the simulation. This analysis provides valuable insights into the protein's collective motions, conformational changes, and

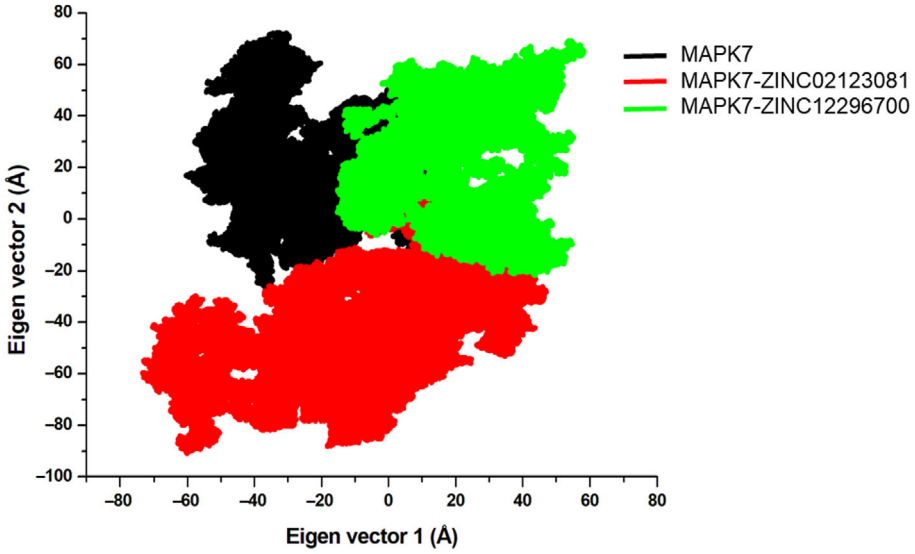

FIGURE 7 Principal component analysis. The graph was constructed by eigenvector 1 versus eigenvector 2 for free mitogen-activated protein kinase 7 (MAPK7), MAPK7-ZINC02123081, and MAPK7-ZINC12296700 after 200 ns of molecular dynamics trajectories.

TABLE 6 MM/GBSA-based binding energy (in kcal/mol) profile of mitogen-activated protein kinase 7 (MAPK7) in complex with ZINC02123081 and ZINC12296700.

Complex	ΔE_{vdW}	ΔE_{ele}	ΔG_{gas}	ΔG_{polar}	$\Delta G_{nonpolar}$	ΔG_{sol}	ΔG_{bind}
MAPK7-ZINC02123081	−35.16	−52.24	−79.01	59.09	−7.14	51.95	−41.09
MAPK7-ZINC12296700	−41.02	−55.11	−81.00	64.27	−4.58	59.69	−48.54

dynamic behavior throughout the simulation. To assess the stability of MAPK7, MAPK7-ZINC02123081, and MAPK7-ZINC12296700, a dynamic approach utilizing PCA was employed. The conformational sampling of the key region is depicted in Figure 7, where the projection is based on the Cα atoms of the systems. The graph illustrates that the substructure of MAPK7 in the complex forms with ZINC12296700 and ZINC02123081 deviates slightly yet shares the same conformational domain as the unbound state. Figure 7 presents the conformational changes of MAPK7 in all three forms: free MAPK7, MAPK7-ZINC02123081, and ZINC12296700-MAPK7. The projection is displayed using two eigenvectors of the covariance matrix. When visualized in a two-dimensional plane, the protein's conformation deviates from its original orientation. There is a small deviation with some overlap among all three systems, as depicted in Figure 7. This enables us to explore the movement pattern of both the bound and unbound states of MAPK7. Overall, the MD simulations and essential dynamics of MAPK7 in complex with ZINC12296700 and ZINC02123081 indicate that they remain stable with minor structural deviations throughout the 200 ns simulations.

3.9 | Molecular mechanics/Poisson–Boltzmann surface area

Precise estimation of the binding affinity of a ligand necessitates consideration of various parameters, among which the solvent condition holds paramount importance.[71] However, the computational molecular docking process did not consider the solvent condition. To account for the solvent's influence and maintain its integrity, we utilized the MM-PBSA approach based on the MD simulation trajectory. We estimated the binding affinity of MAPK7-ZINC02123081 and ZINC12296700-MAPK7 complexes using this method. Table 6 presents the binding energy of the complexes, considering various types of interactions, including van der Waals, electronic, polar, non-polar, solvation, bonded, and non-bonded interactions. The obtained data revealed the Gibbs free energy of binding for the MAPK7-ZINC02123081 and MAPK7-ZINC12296700 complexes to be −41.09 and−48.54 kcal/mol, respectively. These binding free energy values clearly indicate that the MAPK7-ZINC12296700 complex is more stable than the ZINC02123081-MAPK7 complex. The enthalpy of electrostatic and van der Waals interactions exhibited a higher negative magnitude compared to the enthalpy of non-polar interactions in both the MAPK7-ZINC02123081 and ZINC12296700-MAPK7 complexes. This suggests the presence of hydrogen bonds and ionic interactions between MAPK7 and the compounds ZINC02123081 and ZINC12296700. Consequently, this analysis confirms the stability of the MAPK7-ZINC02123081 and MAPK7-ZINC12296700 complexes.

4 | CONCLUSIONS

This study highlights the druggable potential of MAPK7, which plays a crucial role in the progression of various types of cancer. Through a multi-tier virtual screening, we identified two natural compounds,

ZINC02123081 and ZINC12296700, as potent inhibitors of MAPK7. These compounds interacted with key residues within the binding pocket of MAPK7 and demonstrated cancer-inhibitory properties in the PASS analysis. To validate their potential as lead molecules, we performed all-atom MD simulations on MAPK7 in the presence of ZINC02123081 and ZINC12296700. The MM-PBSA analysis further confirmed the stability of the complexes and their significant binding affinities. Computer-aided drug discovery method proves valuable in identifying novel drug-like molecules from natural compounds. Overall, the results indicate that ZINC12296700 and ZINC02123081 possess considerable binding potential toward MAPK7, making them promising candidates for further exploration in drug development targeting cancer. While the study shows promise in identifying potential inhibitors of MAPK7, it is crucial to acknowledge the limitations of computational methods, the need for rigorous in vitro and in vivo validation, and the challenges associated with clinical translation. As we move forward, additional research and clinical validation will be instrumental in further characterizing these compounds' efficacy and safety profiles. Continued investigation may reveal novel insights into their mechanisms of action, potential synergistic effects with existing therapies, and applicability to specific cancer subtypes. With ongoing studies and experimentations, ZINC12296700 and ZINC02123081 may find their place as valuable additions to the arsenal of therapeutic development against cancer in the future.

AUTHOR CONTRIBUTIONS

Conceptualization: Anas Shamsi. Data curation: Lina I. Alnajjar. Formal analysis: Hassan H. Alhassan, Shama Khan, Bandar Alharbi, Nawaf Alshammari, and Mohd Adnan. Funding acquisition: Dharmendra Kumar Yadav and Anas Shamsi. Investigation: Bandar Alharbi, Mohd Adnan, and Anas Shamsi. Methodology: Bandar Alharbi and Anas Shamsi. Project administration: Anas Shamsi. Resources: Shama Khan and Bandar Alharbi. Software: Shama Khan, Nawaf Alshammari, and Mohd Adnan. Validation: Lina I. Alnajjar and Talha Jawaid. Visualization: Hassan H. Alhassan. Writing—original draft: Lina I. Alnajjar, Bandar Alharbi, and Anas Shamsi. Writing—review and editing: Mohd Adnan and Dharmendra Kumar Yadav.

ACKNOWLEDGMENTS

This research was supported by Princess Nourah bint Abdulrahman University Researchers Supporting Project number (PNURSP2023R341), Princess Nourah bint Abdulrahman University, Riyadh, Saudi Arabia.

CONFLICT OF INTEREST STATEMENT

There is no conflict of interest to declare.

DATA AVAILABILITY STATEMENT

The data that supports the findings of this study are available in this articel and associated supplementary material of this article

ORCID

Anas Shamsi https://orcid.org/0000-0001-7055-7056

REFERENCES

1. Manning G, Whyte DB, Martinez R, Hunter T, Sudarsanam S. The protein kinase complement of the human genome. *Science*. 2002; 298(5600):1912-1934.
2. Munk S, Refsgaard JC, Olsen JV, Jensen LJ. From phosphosites to kinases. *Phospho-Proteom Methods Prot*. 2016;1355:307-321.
3. Shchemelinin I, Sefc L, Necas E. Protein kinases, their function and implication in cancer and other diseases. *Folia Biol*. 2006;52(3): 81-100.
4. Kannaiyan R, Mahadevan D. A comprehensive review of protein kinase inhibitors for cancer therapy. *Expert Rev Anticancer Ther*. 2018; 18(12):1249-1270.
5. Tanoue T, Nishida E. Molecular recognitions in the MAP kinase cascades. *Cell Signal*. 2003;15(5):455-462.
6. Buschbeck M, Ullrich A. The unique C-terminal tail of the mitogen-activated protein kinase ERK5 regulates its activation and nuclear shuttling. *J Biol Chem*. 2005;280(4):2659-2667.
7. Yan C, Luo H, Lee J-D, Abe J-i, Berk BC. Molecular cloning of mouse ERK5/BMK1 splice variants and characterization of ERK5 functional domains. *J Biol Chem*. 2001;276(14):10870-10878.
8. Kato Y, Tapping RI, Huang S, Watson MH, Ulevitch RJ, Lee J-D. BMK1/ERK5 is required for cell proliferation induced by epidermal growth factor. *Nature*. 1998;395(6703):713-716.
9. Nakamura K, Johnson GL. PB1 domains of MEKK2 and MEKK3 interact with the MEK5 PB1 domain for activation of the ERK5 pathway. *J Biol Chem*. 2003;278(39):36989-36992.
10. Mody N, Campbell DG, Morrice N, Peggie M, Cohen P. An analysis of the phosphorylation and activation of extracellular-signal-regulated protein kinase 5 (ERK5) by mitogen-activated protein kinase kinase 5 (MKK5) in vitro. *Biochem J*. 2003;372(2):567-575.
11. Raviv Z, Kalie E, Seger R. MEK5 and ERK5 are localized in the nuclei of resting as well as stimulated cells, while MEKK2 translocates from the cytosol to the nucleus upon stimulation. *J Cell Sci*. 2004;117(9): 1773-1784.
12. Drew BA, Burow ME, Beckman BS. MEK5/ERK5 pathway: the first fifteen years. *Biochim Biophys Acta*. 2012;1825(1):37-48.
13. Zhou G, Bao ZQ, Dixon JE. Components of a new human protein kinase signal transduction pathway. *J Biol Chem*. 1995;270(21): 12665-12669.
14. Nithianandarajah-Jones GN, Wilm B, Goldring CE, Müller J, Cross MJ. ERK5: structure, regulation and function. *Cell Signal*. 2012;24(11): 2187-2196.
15. Simoes AE, Rodrigues CM, Borralho PM. The MEK5/ERK5 signalling pathway in cancer: a promising novel therapeutic target. *Drug Discov Today*. 2016;21(10):1654-1663.
16. Krstić J, Trivanović D, Mojsilović S, Santibanez JF. Transforming growth factor-beta and oxidative stress interplay: implications in tumorigenesis and cancer progression. *Oxid Med Cell Longev*. 2015; 2015:1-15.
17. Gavine PR, Wang M, Yu D, et al. Identification and validation of dysregulated MAPK7 (ERK5) as a novel oncogenic target in squamous cell lung and esophageal carcinoma. *BMC Cancer*. 2015;15(1):1-9.
18. Tatake RJ, O'Neill MM, Kennedy CA, et al. Identification of pharmacological inhibitors of the MEK5/ERK5 pathway. *Biochem Biophys Res Commun*. 2008;377(1):120-125. doi:10.1016/j.bbrc.2008.09.087
19. Mody N, Leitch J, Armstrong C, Dixon J, Cohen P. Effects of MAP kinase cascade inhibitors on the MKK5/ERK5 pathway. *FEBS Lett*. 2001;502(1–2):21-24. doi:10.1016/s0014-5793(01)02651-5
20. English JM, Cobb MH. Pharmacological inhibitors of MAPK pathways. *Trends Pharmacol Sci*. 2002;23(1):40-45. doi:10.1016/s0165-6147(00)01865-4
21. Kang C, Kim JS, Kim CY, Kim EY, Chung HM. The pharmacological inhibition of ERK5 enhances apoptosis in acute myeloid leukemia cells. *Int J Stem Cells*. 2018;11(2):227-234. doi:10.15283/ijsc18053

22. Blundell TL. Structure-based drug design. *Nature*. 1996;384(6604 Suppl):23-26.
23. Marrone TJ, Briggs A, James M, McCammon JA. Structure-based drug design: computational advances. *Annu Rev Pharmacol Toxicol*. 1997; 37(1):71-90.
24. Alvarez J, Shoichet B. *Virtual Screening in Drug Discovery*. CRC Press; 2005.
25. Mohammad T, Siddiqui S, Shamsi A, et al. Virtual screening approach to identify high-affinity inhibitors of serum and glucocorticoid-regulated kinase 1 among bioactive natural products: combined molecular docking and simulation studies. *Molecules*. 2020;25(4):823.
26. Khan A, Mohammad T, Shamsi A, et al. Identification of plant-based hexokinase 2 inhibitors: combined molecular docking and dynamics simulation studies. *J Biomol Struct Dynam*. 2021;1–13:10319-10331.
27. Khan MA, Tania M, Fu S, Fu J. Thymoquinone, as an anticancer molecule: from basic research to clinical investigation. *Oncotarget*. 2017; 8(31):51907-51919.
28. Berman HM, Westbrook J, Feng Z, et al. The protein data Bank. *Nucleic Acids Res*. 2000;28(1):235-242. doi:10.1093/nar/28.1.235
29. Roberts RJ. PubMed central: the GenBank of the published literature. *Proc Natl Acad Sci U S A*. 2001;98(2):381-382. doi:10.1073/pnas.98.2.381
30. Daina A, Michielin O, Zoete V. SwissADME: a free web tool to evaluate pharmacokinetics, drug-likeness and medicinal chemistry friendliness of small molecules. *Sci Rep*. 2017;7:42717. doi:10.1038/srep42717
31. Lagunin A, Stepanchikova A, Filimonov D, Poroikov V. PASS: prediction of activity spectra for biologically active substances. *Bioinformatics*. 2000;16(8):747-748. doi:10.1093/bioinformatics/16.8.747
32. Xiong G, Wu Z, Yi J, et al. ADMETlab 2.0: an integrated online platform for accurate and comprehensive predictions of ADMET properties. *Nucleic Acids Res*. 2021;49(W1):W5-W14.
33. Irwin JJ, Shoichet BK. ZINC—a free database of commercially available compounds for virtual screening. *J Chem Inform Model*. 2005; 45(1):177-182. doi:10.1021/ci049714
34. Lill MA, Danielson ML. Computer-aided drug design platform using PyMOL. *J Comput Aided Mol Des*. 2011;25(1):13-19. doi:10.1007/s10822-010-9395-8
35. Mohammad T, Mathur Y, Hassan MI. InstaDock: a single-click graphical user interface for molecular docking-based virtual high-throughput screening. *Brief Bioinform*. 2021;22(4). doi:10.1093/bib/bbaa279
36. Turner P. *XMGRACE Version 5.1. 19. Center for Coastal and Land-Margin Research*. Oregon Graduate Institute of Science and Technology; 2005:2.
37. Lipinski CA. Drug-like properties and the causes of poor solubility and poor permeability. *J Pharmacol Toxicol Methods*. 2000;44(1):235-249. doi:10.1016/s1056-8719(00)00107-6
38. Cavasotto CN, Abagyan RA. Protein flexibility in ligand docking and virtual screening to protein kinases. *J Mol Biol*. 2004;337(1):209-225.
39. Morris GM, Lim-Wilby M. Molecular docking. *Methods Mol Biol*. 2008; 443:365-382. doi:10.1007/978-1-59745-177-2_19
40. Tekade RK. *Basic Fundamentals of Drug Delivery*. Academic Press; 2018.
41. Joseph-McCarthy D, Baber JC, Feyfant E, Thompson DC, Humblet C. Lead optimization via high-throughput molecular docking. *Curr Opin Drug Discov Devel*. 2007;10(3):264-274.
42. Baell JB. Feeling nature's PAINS: natural products, natural product drugs, and pan assay interference compounds (PAINS). *J Nat Prod*. 2016;79(3):616-628. doi:10.1021/acs.jnatprod.5b00947
43. Ramos RS, Macêdo WJC, Costa JS, et al. Potential inhibitors of the enzyme acetylcholinesterase and juvenile hormone with insecticidal activity: study of the binding mode via docking and molecular dynamics simulations. *J Biomol Struct Dyn*. 2020;38(16):4687-4709. doi:10.1080/07391102.2019.1688192
44. Stepanchikova AV, Lagunin AA, Filimonov DA, Poroikov VV. Prediction of biological activity spectra for substances: evaluation on the diverse sets of drug-like structures. *Curr Med Chem*. 2003;10(3):225-233. doi:10.2174/0929867033368510
45. Naqvi AA, Mohammad T, Hasan GM, Hassan M. Advancements in docking and molecular dynamics simulations towards ligand-receptor interactions and structure-function relationships. *Curr Top Med Chem*. 2018;18(20):1755-1768.
46. Pronk S, Páll S, Schulz R, et al. GROMACS 4.5: a high-throughput and highly parallel open source molecular simulation toolkit. *Bioinformatics*. 2013;29(7):845-854. doi:10.1093/bioinformatics/btt055
47. Christen M, Hünenberger PH, Bakowies D, et al. The GROMOS software for biomolecular simulation: GROMOS05. *J Comput Chem*. 2005;26(16):1719-1751. doi:10.1002/jcc.20303
48. van Aalten DM, Bywater R, Findlay JB, Hendlich M, Hooft RW, Vriend G. PRODRG, a program for generating molecular topologies and unique molecular descriptors from coordinates of small molecules. *J Comput Aided Mol Des*. 1996;10(3):255-262. doi:10.1007/bf00355047
49. Shafie A, Khan S, Zehra, Mohammad T, Anjum F, Hasan GM, Yadav DK, Hassan MI. Identification of phytoconstituents as potent inhibitors of casein kinase-1 alpha using virtual screening and molecular dynamics simulations. *Pharmaceutics*. 2021;13(12):2157. doi:10.3390/pharmaceutics13122157
50. Adcock SA, McCammon JA. Molecular dynamics: survey of methods for simulating the activity of proteins. *Chem Rev*. 2006;106(5):1589-1615. doi:10.1021/cr040426m
51. Maisuradze GG, Liwo A, Scheraga HA. Principal component analysis for protein folding dynamics. *J Mol Biol*. 2009;385(1):312-329. doi:10.1016/j.jmb.2008.10.018
52. Ringnér M. What is principal component analysis? *Nat Biotechnol*. 2008;26(3):303-304. doi:10.1038/nbt0308-303
53. David CC, Jacobs DJ. Principal component analysis: a method for determining the essential dynamics of proteins. *Methods Mol Biol*. 2014;1084:193-226. doi:10.1007/978-1-62703-658-0_11
54. Jairajpuri DS, Hussain A, Nasreen K, et al. Identification of natural compounds as potent inhibitors of SARS-CoV-2 main protease using combined docking and molecular dynamics simulations. *Saudi J Biol Sc*. 2021;28(4):2423-2431. doi:10.1016/j.sjbs.2021.01.040
55. Genheden S, Ryde U. The MM/PBSA and MM/GBSA methods to estimate ligand-binding affinities. *Expert Opin Drug Discov*. 2015; 10(5):449-461. doi:10.1517/17460441.2015.1032936
56. Shukla R, Tripathi T. Molecular dynamics simulation of protein and protein–ligand complexes. *In: Singh DB, ed. Computer-Aided Drug Design*. Springer; 2020.
57. Singh S, Baker QB, Singh DB. *Molecular Docking and Molecular Dynamics Simulation*. Elsevier; 2022:291-304.
58. Amir M, Ahmad S, Ahamad S, et al. Impact of Gln94Glu mutation on the structure and function of protection of telomere 1, a cause of cutaneous familial melanoma. *J Biomol Struct Dynam*. 2019;38:1514-1524.
59. Mohammad T, Khan FI, Lobb KA, Islam A, Ahmad F, Hassan MI. Identification and evaluation of bioactive natural products as potential inhibitors of human microtubule affinity-regulating kinase 4 (MARK4). *J Biomol Struct Dynam*. 2019;37(7):1813-1829.
60. Pitera JW. Expected distributions of root-mean-square positional deviations in proteins. *J Phys Chem B*. 2014;118(24):6526-6530.
61. Maruyama Y, Igarashi R, Ushiku Y, Mitsutake A. Analysis of protein folding simulation with moving root mean square deviation. *J Chem Inf Model*. 2023;63(5):1529-1541.
62. Dahiya R, Mohammad T, Roy S, et al. Investigation of inhibitory potential of quercetin to the pyruvate dehydrogenase kinase 3: towards implications in anticancer therapy. *Int J Biol Macromol*. 2019; 136:1076-1085.
63. Naz F, Khan FI, Mohammad T, et al. Investigation of molecular mechanism of recognition between citral and MARK4: a newer therapeutic

approach to attenuate cancer cell progression. *Int J Biol Macromol*. 2018;107:2580-2589.
64. Lobanov MY, Bogatyreva N, Galzitskaya O. Radius of gyration as an indicator of protein structure compactness. *Mol Biol*. 2008;42:623-628.
65. Bizzarri AR, Cannistraro S. *Molecular Dynamics of Water at the Protein–Solvent Interface*. ACS Publications; 2002:6617-6633.
66. Richmond TJ. Solvent accessible surface area and excluded volume in proteins: analytical equations for overlapping spheres and implications for the hydrophobic effect. *J Mol Biol*. 1984;178(1):63-89.
67. Hubbard RE, Haider MK. Hydrogen bonds in proteins: role and strength. *eLS*. 2010.
68. Williams M, Ladbury J. Hydrogen bonds in protein-ligand complexes. *Methods Princ Med Chem*. 2003;19:137.
69. Stein SAM, Loccisano AE, Firestine SM, Evanseck JD. Principal components analysis: a review of its application on molecular dynamics data. *Ann Rep Comput Chem*. 2006;2:233-261.
70. Papaleo E, Mereghetti P, Fantucci P, Grandori R, De Gioia L. Free-energy landscape, principal component analysis, and structural clustering to identify representative conformations from molecular dynamics simulations: the myoglobin case. *J Mol Graph Model*. 2009;27(8):889-899.
71. Miller BR III, McGee TD Jr, Swails JM, Homeyer N, Gohlke H, Roitberg AE. MMPBSA. Py: an efficient program for end-state free energy calculations. *J Chem Theor Comput*. 2012;8(9):3314-3321.

SUPPORTING INFORMATION

Additional supporting information can be found online in the Supporting Information section at the end of this article.

How to cite this article: Alharbi B, Alnajjar LI, Alhassan HH, et al. Identification of mitogen-activated protein kinase 7 inhibitors from natural products: Combined virtual screening and dynamic simulation studies. *J Mol Recognit*. 2024;37(1):e3067. doi:10.1002/jmr.3067